Flux-closure pattern in a two-dimensional NbN–Fe superconductor-ferromagnet nanocomposite: Anisotropy of the angular magnetoresistance

S. K. Bose[1] and R. C. Budhani[1,2,a)]
[1]*Department of Physics, Condensed Matter–Low Dimensional Systems Laboratory, Indian Institute of Technology Kanpur, Kanpur 208016, India*
[2]*National Physical Laboratory, Dr. K. S. Krishnan Marg, New Delhi 110012, India*

(Received 15 July 2010; accepted 1 October 2010; published online 30 November 2010)

The angular dependence of magnetoresistance (MR) of distributed NbN–Fe–NbN Josephson-junctions in the out-of-plane and in-plane magnetic field geometries shows a striking anisotropy on the polarity of the current (I_+/I_-) and its direction with respect to the applied field. The origin of this anisotropy is suggested to be the difference in the degree of spin polarization of electrons injected from Fe nanoplaquettes into the superconducting NbN for I_+ and I_-. Such a conclusion is based on the topography of flux-closure domains in Fe plaquettes. The anisotropy of MR is suppressed at high fields as the flux-closure domains transform into a single-domain structure. © *2010 American Institute of Physics*. [doi:10.1063/1.3510590]

I. INTRODUCTION

The extent of supercurrent transport through a nonsuperconducting layer separating two massive superconductors (SCs) depends sensitively on the electrical and magnetic character of the former. For insulating layers, the supercurrent decays rapidly as the layer thickness exceeds a few tens of angstroms.[1] For nonmagnetic metal barriers, the proximity induced pair correlations allow the supercurrent propagation over distances as large as few microns.[2] The supercurrent transport and magnetic screening response of such proximity coupled Josephson-junction (JJ) ensembles, ordered or otherwise, have been studied extensively.[3–8] In absence of magnetic fields, coupled JJs in two-dimension (2D) approach zero resistance state via Kosterlitz–Thouless (KT) transition[9] at T_{KT}. Increasing the temperature above T_{KT}, dissociates the vortex-antivortex bound pairs and the resultant increase in entropy leads to some finite resistance.[4] Below T_{KT}, vortices introduced by a small external magnetic field are mobile. The mobility of such vortices is manifested as a broadened resistive transition.

An exciting new dimension is added to the problem of proximity coupled JJs when the barrier metal is a ferromagnet (FM).[10–13] Single JJs with magnetic barriers have been studied in recent years and effects such as oscillating critical current[14,15] and long range proximity effect suggesting a singlet-to-triplet conversion at the junction interface,[16] have been observed. An important factor which affects the response of an FM-SC heterostructure is the behavior of magnetic domain walls (DW) in the FM layer. The DW motion can be induced by external magnetic fields,[17] sufficiently high (spin-polarized) currents,[18,19] and current pulses.[20,21]

In a recent letter,[22] we reported briefly the successful self-assembly of distributed NbN–Fe–NbN JJs by stress-tuned Volmer–Weber type plaquette growth of Fe on [100] MgO, whose electrical connectivity is then tailored by NbN overlayers of different thickness (d_{NbN}). The critical current density $J_c(T)$ showed signatures of transport in random assembly of JJs. The present paper is an extension of that letter.[22] Here, we address how the magnetic-flux-closure domains of Fe plaquette affect Josephson coupling between NbN layers through careful measurements of the angular dependence of magnetoresistance (MR) in the superconducting transition regime. We also address the granular nature of transport in such systems through ac-susceptiblity measurements. These new measurements bring out the contribution of magnetic DW motion triggered by external magnetic field in controlling the Cooper pair transport in such distributed JJs.

II. EXPERIMENT

The samples studied here consist of Fe nanoplaquettes covered with superconducting NbN, prepared by pulsed laser deposition technique. Films were prepared by ablation of Fe and Nb targets by a KrF excimer laser ($\lambda=248$ nm) in a all-metal-seal chamber at 700 °C and 200 °C, respectively, on [100] MgO substrate. Further details of film preparation are given elsewhere.[22,23] The Fe layer was deposited first to a nominal thickness of ≈40 nm. This was followed by NbN overlayer of thickness 10, 20, and 30 nm. The morphology investigated via scanning electron microscopy (SEM) and atomic force microscopy (AFM) revealed the underlying mesoscopic structure. The x-ray fluorescence mapping and $\theta-2\theta$ x-ray diffraction (resolution ≈18 arcsec) were performed to confirm the formation of Fe plaquettes and nature of NbN coverage on the underlying Fe structure. The electronic transport measurements in a four-probe geometry were performed on bridges of $\approx 75\times 1300$ μm^2 area fabricated by Ar^+ ion milling. Angular dependence of MR with magnetic field (H) rotated in-plane and also out-of-plane geometries brought out some very unique and interesting aspects of supercurrent transport in such JJ ensembles.

The temperature dependence of interplaquette critical current density has been investigated by isothermal field dependent ac-susceptiblity ($\chi=\chi'+i\chi''$) measurements.[24,25] The

a)Electronic addresses: rcb@iitk.ac.in and rcb@mail.nplindia.ernet.in.

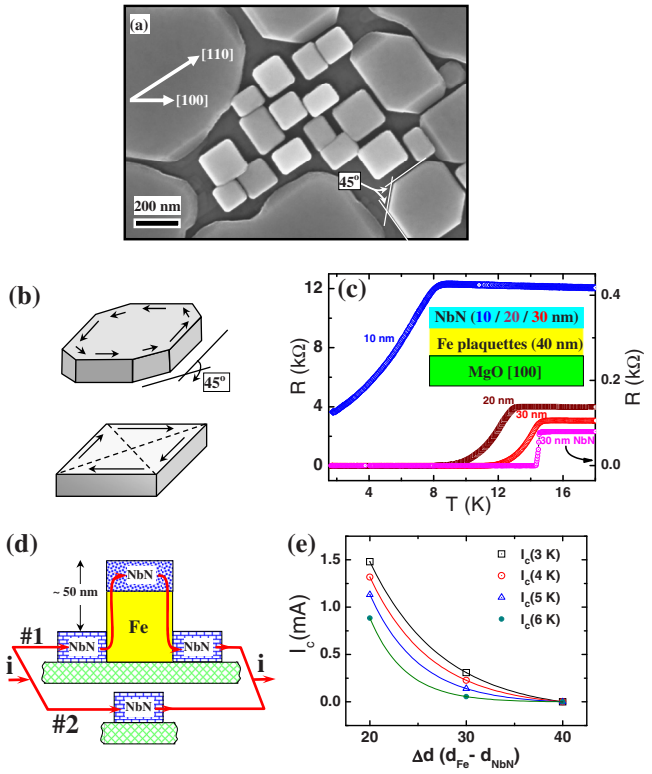

FIG. 1. (Color online) (a) Scanning electron micrograph of the Fe (40 nm)/NbN (30 nm) sample showing the formation of nearly square Fe plaquettes of $\approx 100 \times 100$ nm^2 area, separated by ≈ 20 nm gaps and are aligned along MgO [110] direction. Apart from these distributed square plaquettes, there is also formation of bigger ($\approx 250 \times 250$ nm^2) faceted rectangular plaquettes with facet angle of 45°. (b) Schematic illustration of magnetic domain structure indicating magnetic-flux-closure pattern. (c) Resistances of the 10/20/30 nm Fe–NbN hybrids (left Y scale) measured as a function of temperature, along with the resistance of a 30 nm plain NbN film (right Y scale). (d) A sketch depicting the two distinct parallel paths for the flow of supercurrent through Fe–NbN hybrids. Path 1 is the double JJ path, i.e., through NbN–Fe–NbN junctions, where as path 2 is for current flow through the interplaquette NbN forming a percolating backbone. (e) The variation in critical current (I_c) with $\Delta d = d_{Fe} - d_{NbN}$ at 3, 4, 5, and 6 K. Solid lines are fits to first order exponential decrease.

screening current response to alternating magnetic field perpendicular to the film plane contains vital information about the strength of induced shielding currents and energy dissipation in the material. A custom-made single coil susceptometer, which makes use of a 25×25 μm^2 Hall probe,[26] has been employed for these measurements. Magnetization measurements were performed using a Quantum Design make superconducting quantum interference device.

III. RESULTS AND DISCUSSION

Figure 1(a) shows one typical SEM of the 30 nm Fe–NbN sample [Fe (40 nm)/NbN (30 nm)]. The formation of nearly perfect square Fe plaquettes of $\approx 100 \times 100$ nm^2 area, separated by ≈ 20 nm gaps and aligned along MgO [110] direction is evident from the figure. The deposition of NbN at reduced temperatures (200 °C) leads to the NbN coverage on top of the Fe plaquettes as well as in the interplaquette spaces, as depicted in Fig. 1(d) and has been confirmed via x-ray fluorescence mapping of niobium. Since the NbN layer thickness is ≤ 30 nm and the Fe plaquettes are ≈ 50 nm high (confirmed via AFM line scan) with nearly perfect vertical walls, there is absence of any direct contact between the inter- and intraplaquette NbN. In addition to the small square plaquettes, there is also formation of bigger ($\approx 250 \times 250$ nm^2) faceted rectangular plaquettes with facet angle of 45°. This angle matches with the facet angle of Fe islands with magnetic-flux-closure,[27,28] leading to in-plane flux-confinement in such a way that there is very small ferromagnetic exchange interaction between them [Fig. 1(b)]. For magnetic nanostructures, there exists a critical size above which the magnetostatic energies dominate over the anisotropy energies leading to flux-closure domains. This so called single-domain limit has been predicted by micromagnetic calculations and is supported by magnetic imaging techniques.[29,30] The aspect ratio of Fe nanoplaquettes studied in our case is appropriate for creation of magnetic vortex with flux-closure-domains.

The superconducting transition of the SC-FM hybrids is shown in Fig. 1(c), along with the SC-transition of a plain 30 nm thick NbN film. The normal state resistance (R_n) of the hybrids increases with decrease in temperature, highlighting the strongly granular character of the structure. Reduction in NbN layer thickness from 30 to 10 nm leads to substantial drop in the transition temperature (T_c) along with increase in the width of the transition (ΔT_c). Interestingly, inspite of the R_n of the hybrid with 30 nm thick NbN being 3 orders of magnitude larger than the R_n of pure NbN film, the superconducting onset temperature (T_{onset}) remains nearly the same (≈ 14.7 K). The ΔT_c(≈ 2 K) of this hybrid, however, is seven times higher than that of pure NbN (≈ 0.3 K), suggesting that the superconductivity in interplaquette epitaxial NbN sets in at ≈ 14.7 K but zero resistance state appears only when the intraplaquette NbN (on top of the Fe plaquettes) goes superconducting at ≈ 11 K. This lower value of T_c for intraplaquette NbN is suggestive of exchange field-induced depairing and the strain at NbN–Fe interface. The normal state resistivity (ρ_n) for plain 30 nm NbN is ~ 22 $\mu\Omega$ cm, which is nearly an order of magnitude larger than that of bulk Fe at 20 K (~ 2 $\mu\Omega$ cm).[31] However, the presumably large resistance of the vertical interfaces between NbN and Fe lead to this enhanced R_n of Fe–NbN (30 nm) system in comparison to the R_n of plain 30 nm NbN system. On the other hand, we do not expect the lateral interface between Fe and top NbN to be very resistive.

The complex ac-susceptibility (χ) measurement is another important tool to investigate the strength and dynamics of intergrain and intragrain coupling in granular SCs.[32] Application of a very small perpendicular ac magnetic field (h_{ac}) to a planar SC does not introduce any new vortices, which may lead to weakening of the complete Meissner state. The superfluid, however, responds to screen-out the external field by switching rapidly from clockwise to counterclockwise flow. For a granular SC, this leads to inter- and intragrain energy losses, manifesting in the real and imaginary part of the pickup voltage. The imaginary part of the locked-in voltage signal from the Hall probe in the present case is directly proportional to imaginary part of susceptibility (χ''). In granular SCs, χ'' has two distinct peaks. As shown by Clem and Sanchez,[32] the low-field peak in χ'' is

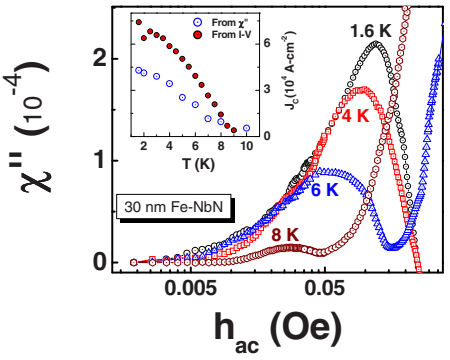

FIG. 2. (Color online) Variation in the imaginary part of complex ac-susceptibility (χ'') with magnitude of perpendicular ac magnetic field (h_{ac}) at different temperatures. The low-field peak is caused by the granular nature of superconductivity in the nanocomposite. A comparison of critical current density measured from transport and inferred from χ measurements is plotted in the inset.

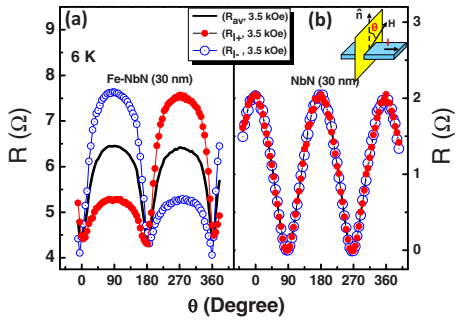

FIG. 4. (Color online) (a) Variation in sample resistance at 6 K of a Fe–NbN sample (30 nm NbN) as the angle between the field (3.5 kOe) and sample normal (N) is changed from 0° to 360°. A striking anisotropy of R is seen clearly for two polarities (I_+ and I_-) of the current. (b) The angular dependence of resistance of a plain 30 nm NbN film, shows R being independent of the relative direction of current with magnetic field. Inset of (b) shows a sketch of measurement geometry. The current flows along [100] direction.

caused by intergrain losses, whereas the higher field peak is linked to intragrain losses. The intergrain critical current density of a sample of thickness d is given in terms of the ac field magnitude (h_{ac}^j) at which the low-field peak in χ'' appears as,

$$J_{cj}(T) = h_{ac}^j/(1.942d/2). \quad (1)$$

Figure 2 shows the field dependence of χ'' of Fe–NbN hybrids with 30 nm thick NbN layer, indicating the low-field peak at different temperatures. The $J_{cj}(T)$ calculated from the peak position is plotted against T in the inset of Fig. 2 along with the J_c calculated from transport measurements with a voltage criterion of 100 μV/cm. Although, this $J_{cj}(T)$ is slightly underestimated in comparison to the $J_c(T)$ calculated from transport measurement, they have a compatible temperature dependence.

To know the magnetic state of the islands, magnetization (M) measurements were performed at 5 K with field (H) applied in-plane as well as perpendicular to the plane of the film. Figure 3 shows the result of these $M-H$ measurements. A quick saturation of magnetization for in-plane field indicates that the films have in-plane anisotropy. The $M-H$ loop also shows low coercivity (~60 Oe) along with a low remanence factor (~0.06), in agreement with the earlier studies of isolated Fe islands.[33]

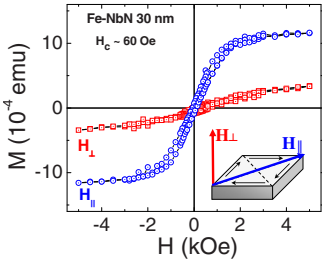

FIG. 3. (Color online) Magnetization of the 30 nm NbN covered Fe plaquettes measured at 5 K with field-in-plane (open circles) and out-of-plane (open squares) configurations. The data have been corrected for the linear diamagnetic contribution of the substrate. The coercive field is ~60 Oe for the in-plane measurement. The lower inset shows the direction of the perpendicular and parallel fields on the plane of the plaquette.

The effect of magnetic field on the superconducting state of the hybrids has been investigated via angular dependence of MR measurements. These have been performed by rotating the direction of the magnetic field with respect to the plane of the sample, as shown in the inset of Fig. 4. One typical MR response of 30 nm Fe–NbN sample, obtained at 6 K is presented in Fig. 4(a), along with that of a plain 30 nm thick NbN film, as shown in Fig. 4(b). The data in Figs. 4(a) and 4(b) have been plotted for different directions of current (I); I_- (open circle), I_+ (closed circle), and $I_{av}[R_{av}=(R_{I+}+R_{I-})/2]$ (bold line). There are two characteristics features of the data for Fe–NbN hybrids in stark contrast to the data for the plain NbN film. First, both I_+ and I_- show an enhanced resistance (R) when the field (3.5 kOe) is in the plane of the film (θ=90° and 270°), as compared to the resistance for θ=0° and 180°. Which is not the case for plain NbN film, where enhanced dissipation is seen at θ=0° and 180°. Second, at θ=90°, R_{I-} is much larger than R_{I+}, whereas at θ=270°, $R_{I-} \ll R_{I+}$. To rule out the possibility that this unconventional behavior of $R(\theta)$, could be an artifact of thermal gradients, the measurement was repeated by reversing the direction of magnetic field and polarity of the current. The asymmetry of the peak in resistance at 90° and 270° for I_+ and I_- remains. In contrast, the MR response of a plain NbN film is independent of the direction of the electronic flow [Fig. 4(b)]. Here it is important to mention that in our experiment the sample stays stationary, whereas the magnet is rotated. Hence, the asymmetry of R cannot be an artifact of sample rotation and associated noise.

In order to understand the current polarity dependence of the anisotropic MR, we analyze the roles of the relevant channels available for supercurrent transport in the hybrid. The unique structure of the plaquettes allows the flow of supercurrent through two parallel channels as shown in Fig. 1(d). One of these paths (labeled #1) is the double S-F-S junction, and the other route (#2) is the thin percolating backbone of NbN in the interplaquette spaces. The critical current (I_c) follows $(1-T/T_c)$ and $(1-T/T_c)^{1/2}$ dependence for $T \approx T_c$ and $T \ll T_c$, respectively,[22] in accordance with the theory of supercurrent transport in such JJs.[34] This observation suggests path #1 as the dominant channel for transport.

In case, the interplaquette epitaxial NbN (path #2) were to dominate the supercurrent transport, the I_c should follow the Ginzburg–Landau dependence of the type $\sim(1-T/T_c)^{3/2}$ throughout the temperature range.[25] Even in the case of a transition from Ginzburg–Landau to Ambegaokar–Baratoff regime,[35] due to granularity in the system, the I_c would vary as $(1-T/T_c)^{3/2}$ near T_c and $(1-T/T_c)^{1/2}$ at $T \ll T_c$, which is not the case here. The I_c instead follows a $(1-T/T_c)$ dependence near T_c. The variation in I_c at different temperatures also show monotonic decrease with the relevant FM thickness $\Delta d(=d_{\mathrm{Fe}}-d_{\mathrm{NbN}})$, as been presented in Fig. 1(e). However, the expected first order exponential fits (solid lines) are rather inconclusive due to availability of only three data points corresponding to 10, 20, and 30 nm NbN thickness. Furthermore, it may still be argued that the current never enters the top intraplaquette NbN to form the JJ. While this scenario of current just passing through the Fe plaquette length is plausible, it is highly unlikely. The reason lies in the very large width to thickness ratio of the plaquettes ($\sim$200 nm/50 nm) and the superconducting nature of NbN, which will short the current path through Fe. The establishment of S-F-S channel for transport explains the large dissipation for in-plane-field as the phase of the tunneling order parameter for double NbN–Fe–NbN channel is affected significantly when the field is in the plane of the junctions. This is in contrast to the case of plain SC films where it is the out-of-plane field which contributes significantly to dissipation, due to the plenitudinous motion of Abrikosov vortices.

For further understanding the current direction dependence of $R(\theta)$ response, we have also measured the change in resistance $[R(\Phi)]$ as the magnetic field is rotated in the plane of the film. One such measurement at 6 K for I_+ and I_- is shown in Fig. 5(a). The average response $[(R_{I+}+R_{I-})/2]$ (bold line) peaks when H is perpendicular to I ($\Phi=90°$ and 270°). However, the R_{I+} and R_{I-} separately show large asymmetry in response at $\Phi=90°$ and 270°. We believe that the reason for this striking behavior lies in magnetic domain structure of the Fe plaquettes. Figure 5(b) shows a schematic view of the magnetic-flux-closure domains of one Fe plaquette in zero field. The direction of current is also marked in the figure. In the absence of external field, the individual magnetic domains are of equal strength, with magnetization rotated by $\pi/2$ across the DW. In Fig. 5(b), we also show a cross section of the Fe plaquette along the line PQ drawn on its top view. The $\pi/2$ rotated domains of the plaquette are shown as hatched areas. As the electrons climbs up these areas into the top NbN layer, they get spin-polarized. In zero field, the hatched areas of magnetization angle Ψ and $\Psi+\pi/2$ are equal. The same is the case for a nonzero field H provided $\Phi=0°$ as shown in Fig. 5(c). In this case, the current travels equal areas of $\pi/2$ out-of-phase domains while entering and exiting the top NbN. Thus, we expect a fixed value for resistance due to pair breaking effects in NbN irrespective of the polarity of current. However, when $\Phi=90°$ or 270° as shown in Figs. 5(d) and 5(e), respectively, the magnetic domains grow in the direction of H at the expense of the ones with nonzero antiparallel component of $\vec{M}$. Thus, for Fig. 5(d), we argue that the electrons injected by I_- to be strongly spin-polarized ($P_{I+}<P_{I-}$), resulting in enhancement of R_{I-}. Whereas, the ones injected by I_+ in this scenario are weakly spin-polarized (due to intervening DW), therefore, the resistance decreases with increasing Φ. At $\Phi=270°$ [Fig. 5(e)], the domains grow in the direction reverse of what is seen in Fig. 5(d), and thus the resistance goes through a minimum for I_-. The angular (Φ) dependence of R for in-plane field as discussed above, also explains the anisotropic out-of-plane field response (Fig. 4). In the θ range of 0°–90° the horizontal component of magnetic field ($H \sin\theta$) leads to the DW motion and thus the unequal resistance values for I_+ and I_-.

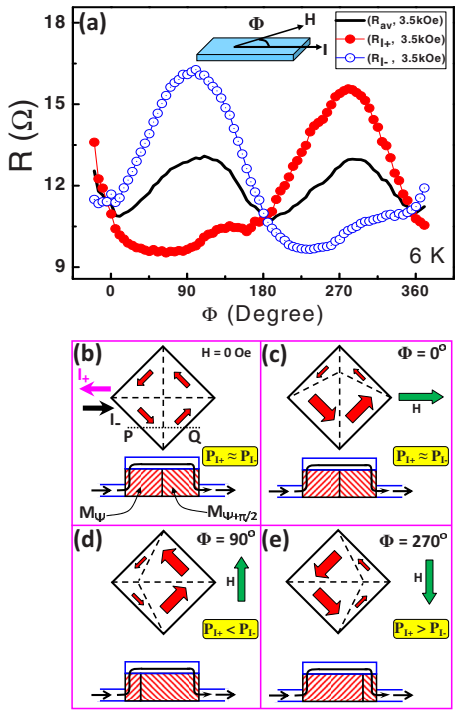

FIG. 5. (Color online) (a) Angular dependence of resistance at 6 K in the presence of in-plane magnetic field (3.5 kOe) applied at angle Φ with respect to the direction of current. The measurement geometry is shown in the inset. The variation in $R(\Phi)$ depends critically on the polarity of current. [(b)–(e)] Magnetic flux-closure domains of Fe nanoplaquettes aligned at an angle $\approx\pi/4$ with respect to field direction grows at the expense of the domains with angle $\approx 3\pi/4$. This leads to unequal spin polarization for I_+ and I_- leading to anisotropic angular dependence. The effect is maximum at $\Phi=\pi/2$ and $3\pi/2$. Lower sketch in (b)–(e) shows the cross-section of Fe plaquettes along the line PQ.

It would be appropriate here to address how the magnetism of Fe plaquettes affects the supercurrent transport through the percolating NbN path. Although the magnetic-flux-closure domains would restrict the leakage of magnetic-flux into the interplaquette NbN, exchange field of the FM would certainly weaken the superconducting order parameter, and hence lead to Josephson coupling across the plaquettes. However, we feel that the complete randomness of current flow pattern (percolating path i.e., #2) would washout any current polarity dependence of MR.

To decouple the contributions of the "dephasing of S-F-S coupling" and "magnetic domain growth by external field" on $R(H)$, we have measured the temperature dependence of the out-of-plane MR response in 3.5 kOe field. These data are presented in Fig. 6(a) for both I_+ and I_-. We note that at 16 K [above T_c, bottom curve in Fig. 6(a)], the sample resis-

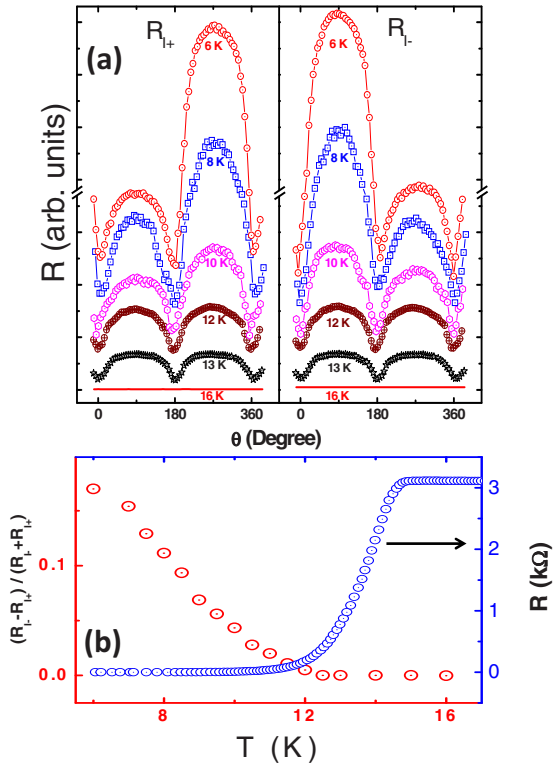

FIG. 6. (Color online) (a) The angular (θ) dependence of sample resistance measured at several temperatures in 3.5 kOe field. The graphs have been vertically shifted (indicated by line-breaks) for better visual representation. Here, θ is the angle between field direction and film normal. Angular dependence of resistance for both I_+ and I_- are shown. (b) Relative difference in R_{I+} and R_{I-} is maximum at θ=90°. It is plotted as a function of temperature along with resistance of the sample in zero field. The polarity dependence of resistance emerges only below ~11 K, at which the zero field resistance goes to zero.

tance has no discernible angular dependence, and at 13 and 12 K, the peak value for R at θ=90° and 270° is the same for I_+ and I_-. However, as the temperature is lowered below ≈11 K, the asymmetry of R at θ=90° or 270° and the difference in R_{I+} and R_{I-} start emerging and become increasingly prominent at lower temperatures. To highlight this effect, in Fig. 6(b), we plot the behavior of $(R_{I-}-R_{I+})/(R_{I-}+R_{I+})$ at θ=90°, as a function of temperature. The plot also shows the variation in sample resistance as a function of temperature. A zero resistance state is established only below $T \approx 11$ K. We have argued earlier that the NbN layer on top of Fe plaquettes has a lower critical temperature presumably due to the exchange field of the Fe and also lattice mismatch induced strain. This view is supported by the observation of a fully superconducting state at $T \leq 11$ K. Thus, the explanation presented earlier for asymmetry of R_{I+} and R_{I-} in the framework of pair breaking by spin-polarized electrons is relevant only when the top NbN becomes superconducting.

If the dissimilarity of R_{I+} and R_{I-} at $T \leq 11$ K is due to the growth of Ψ and $\Psi-\pi/2$ flux-closure domains at the expense of $\Psi+\pi/2$ and $\Psi+\pi$ domains as shown in Fig. 5, then at sufficiently large fields, where the plaquette becomes a single-domain entity, the inequality of R_{I+} and R_{I-} must disappear. To see whether this happens or not, we have measured $R(\theta)$ at 6 K for different values of the magnetic field. The results of this measurement are shown in Fig. 7. Here,

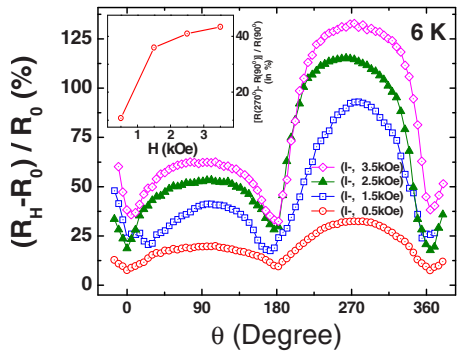

FIG. 7. (Color online) MR in percentage as a function of the angle θ at 6 K for positive polarity of the current. Data are taken at several values of field strength for the same I_+. As presented in the inset, anisotropy in peak MR value $[R(270°)-R(90°)/R(90°)]$ gets saturated at higher fields. At sufficiently high field this asymmetry would vanish, as then the magnetic-vortex-state gives way to a single-domain-state.

we have plotted the MR defined as $(R_H-R_0)/R_0$ in percentage, where R_H and R_0 are the resistances of the sample in presence of field H and in zero field, respectively. We note that the difference in the height of the peaks at θ=90° and 270°, first grows rapidly with field and then starts tapering off. In principle, this difference should go to zero when the plaquette becomes a single-domain at very high fields. Such a situation is not reached in our case due to a limited H(≈3.5 kOe) available to us. There is also a possibility that due to edge effects, the required field may be much larger than the saturation field of magnetic hysteresis measurement. It is also important to stress that the resistance values at the lowest points (θ=0°, 180°, and 360°), which correspond to field perpendicular to the film plane, increase with the strength of the external field. This is primarily due to the increased number density of Abrikosov vortices in the film.

IV. CONCLUSIONS

In summary, we have observed a strong anisotropy in the current direction dependence of dissipation in a 2D nanocomposite of Fe and NbN bilayers. This composite consists of well separated, nearly square Fe nanoplaquettes grown on [100] MgO and then covered with NbN of varying thickness (10, 20, and 30 nm). The critical current density $J_c(T)$ and ac screening response of this unique structure has signature of a distributed JJ array. The angular dependence of resistance in out-of-plane and in-plane geometries depends upon the Josephson coupling of the two NbN layers via Fe plaquettes, and relative direction of electronic flow and magnetic field. It is argued that the DW motion induced by the in-plane component of the magnetic field leads to a different degree of spin polarization of the electrons injected into the intra-plaquette NbN for the current of opposite polarity. The anisotropy of $R(H)$ for I_+ and I_- saturates at higher magnetic fields. It is predicted that this anisotropy would completely vanish at very high fields, as then the flux-closure pattern will give way to a single-domain structure.

ACKNOWLEDGMENTS

This research has been supported by grants from the Department of Science & Technology under its Nanoscience & Nanotechnology initiative and by the Board for Research in Nuclear Science. S. K. Bose acknowledges financial support from the Council for Scientific and Industrial Research, Government of India. Technical help of Pooran C. Joshi is acknowledged.

[1]J. C. Fisher and I. Giaever, J. Appl. Phys. **32**, 172 (1961).
[2]K. K. Likharev, Rev. Mod. Phys. **51**, 101 (1979).
[3]L. L. Sohn, M. S. Rzchowski, J. U. Free, and M. Tinkham, Phys. Rev. B **47**, 967 (1993).
[4]C. J. Lobb, D. W. Abraham, and M. Tinkham, Phys. Rev. B **27**, 150 (1983).
[5]W. A. C. Passos, F. M. Araujo-Moreira, and W. A. Ortiz, J. Appl. Phys. **87**, 5555 (2000).
[6]M. S. Rzchowski, S. P. Benz, M. Tinkham, and C. J. Lobb, Phys. Rev. B **42**, 2041 (1990).
[7]M. Tesei and R. Théron, EPL **85**, 67005 (2009).
[8]M. Tinkham, *Introduction to Superconductivity*, 2nd ed. (McGraw-Hill, New York, 1996), p. 239.
[9]J. M. Kosterlitz and D. J. Thouless, J. Phys. C **6**, 1181 (1973).
[10]A. V. Veretennikov, V. V. Ryazanov, V. A. Oboznov, A. Y. Rusanov, V. A. Larkin, and J. Aarts, Physica B **284–288**, 495 (2000).
[11]S. Takahashi, T. Yamashita, T. Koyama, S. Maekawa, and H. Imamura, J. Appl. Phys. **89**, 7505 (2001).
[12]T. Kontos, M. Aprili, J. Lesueur, F. Genêt, B. Stephanidis, and R. Boursier, Phys. Rev. Lett. **89**, 137007 (2002).
[13]J. W. A. Robinson, S. Piano, G. Burnell, C. Bell, and M. G. Blamire, Phys. Rev. B **76**, 094522 (2007).
[14]A. I. Buzdin, M. Y. Kupriyanov, and B. Vujicic, Physica C **185–189**, 2025 (1991); Sov. Phys. JETP **74**, 124 (1992).
[15]V. V. Ryazanov, V. A. Oboznov, A. Yu. Rusanov, A. V. Veretennikov, A. A. Golubov, and J. Aarts, Phys. Rev. Lett. **86**, 2427 (2001).
[16]R. S. Keizer, S. T. B. Goennenwein, T. M. Klapwijk, G. Miao, G. Xiao, and A. Gupta, Nature (London) **439**, 825 (2006).
[17]G. S. D. Beach, C. Nistor, C. Knutson, M. Tsoi, and J. L. Erskine, Nature Mater. **4**, 741 (2005).
[18]F. J. Albert, J. A. Katine, R. A. Buhrman, and D. C. Ralph, Appl. Phys. Lett. **77**, 3809 (2000).
[19]M. Tsoi, R. E. Fontana, and S. S. P. Parkin, Appl. Phys. Lett. **83**, 2617 (2003).
[20]L. Berger, J. Appl. Phys. **71**, 2721 (1992).
[21]M. Yamanouchi, D. Chiba, F. Matsukura, and H. Ohno, Nature (London) **428**, 539 (2004).
[22]S. K. Bose and R. C. Budhani, Appl. Phys. Lett. **95**, 042507 (2009).
[23]S. K. Bose, R. Sharma, and R. C. Budhani, Phys. Rev. B **78**, 115403 (2008).
[24]L. K. Sahoo, S. Patnaik, R. C. Budhani, and W. L. Holstein, Phys. Rev. B **63**, 214501 (2001).
[25]K. Senapati, N. K. Pandey, R. Nagar, and R. C. Budhani, Phys. Rev. B **74**, 104514 (2006).
[26]K. Senapati, S. Chakrabarty, L. K. Sahoo, and R. C. Budhani, Rev. Sci. Instrum. **75**, 141 (2004).
[27]R. Hertel, O. Fruchart, S. Cherifi, P.-O. Jubert, S. Heun, A. Locatelli, and J. Kirschner, Phys. Rev. B **72**, 214409 (2005).
[28]P.-O. Jubert, J.-C. Toussaint, O. Fruchart, C. Meyer, and Y. Samson, Europhys. Lett. **63**, 132 (2003).
[29]A. Yamasaki, W. Wulfhekel, R. Hertel, S. Suga, and J. Kirschner, Phys. Rev. Lett. **91**, 127201 (2003).
[30]R. P. Cowburn, D. K. Koltsov, A. O. Adeyeye, M. E. Welland, and D. M. Tricker, Phys. Rev. Lett. **83**, 1042 (1999).
[31]P. Granberg, P. Isberg, T. Baier, B. Hjörvarsson, and P. Nordblad, J. Magn. Magn. Mater. **195**, 1 (1999).
[32]J. R. Clem and A. Sanchez, Phys. Rev. B **50**, 9355 (1994).
[33]T. Zhu and Y. J. Wang, Phys. Rev. B **60**, 11918 (1999).
[34]A. I. Buzdin and M. Y. Kupriyanov, Pis'ma Zh. Eksp. Teor. Fiz. **53**, 308 (1991) [JETP Lett. **53**, 321 (1991)].
[35]J. R. Clem, B. Bumble, S. I. Raider, W. J. Gallagher, and Y. C. Shih, Phys. Rev. B **35**, 6637 (1987).